Environ. Sci. Technol. **2001**, *35,* 398−405

Photocatalytic Degradation of Selected s-Triazine Herbicides and Organophosphorus Insecticides over Aqueous TiO_2 Suspensions

IOANNIS K. KONSTANTINOU, THEOPHANIS M. SAKELLARIDES, VASILIS A. SAKKAS, AND TRIANTAFYLLOS A. ALBANIS*

Department of Chemistry, University of Ioannina, Ioannina 45110, Greece

The photocatalytic degradation of selected s-triazine herbicides and organophosphorus insecticides was carried out in aqueous TiO_2 suspensions under simulated solar light. The tested herbicides from the s-triazines group were atrazine, propazine, cyanazine, prometryne, and irgarol. The tested insecticides from the organophosphorus group were ethyl parathion, methyl parathion, ethyl bromophos, methyl bromophos, and diclofenthion. Degradation kinetics followed first-order reaction and has been monitored through gas chromatography. The degradation was fast with half-lives varying from 10.2 to 38.3 min depending on the nature and the structure of compounds. The generated transformation products (TPs) were formed via oxidation, dealkylation, and dechlorination for s-triazines and via oxidation and photohydrolysis for organophosphates. The TPs of irgarol, bromophos, and dichlofenthion were identified using solid-phase extraction (SDB-disks) and GC-MS techniques, and possible degradation routes were proposed showing similar degradation pathways as for other triazines and organophosporus pesticides. This work points out to the necessity of extended knowledge of the successive steps in a solar-assisted detoxification process.

Introduction

Since pesticides as s-triazines and organophosphates are widely used for weed and insect control in agricultural crops, their behavior in the environment is vitally important. s-Triazines are used as pre- and postemergence herbicides for the control of annual and perennial grass and annual broad-leaved weeds. The potential for contamination of water and sediment samples is high owing to their physicochemical properties such as water solubility, adsorptivity (K_{oc}), and hydrolysis half-lives (>25 weeks) (*1*). The herbicide 2-(methylthio)-4-(*tert*-butylamino)-6-(cyclopropylamino)-s-triazine (tradename Irgarol 1051) is widely used in antifouling paints as a biocide agent in substitution to the tributyltin (TBT) and copper-based agents. The herbicide is used as an alternative additive in paints in order to reduce primary colonization by algae and growth of seaweeds in boats (*2, 3*). As a result of its low solubility (7 mg/L) and high hydrophobicity (K_{ow} = 3.95) was detected in European lake, estuarine, and coastal waters (*3*−*6*).

* Corresponding author phone: +30 651 98348; fax: +30 651 98795; e-mail: talbanis@cc.uoi.gr.

The organophosphorus insecticides are comprised within the 10 most widely used pesticides all over the world. They are applied in different types of cultivation for the elimination of custaceans, fruit flies, and mosquitoes (*7*). These compounds are extremely toxic, acting on acetylcholinesterase activity. Residue levels of organophosphorus insecticides have been reported in environmental waters (*8, 9*).

As a result, effective purification methods for eliminating pesticides in natural waters have been in urgent demand. Degradation and purification processes for polluted waters include adsorption on various adsorbents (*10*−*12*) and especially on activated carbon (*12*), microbial action (biodegradation) (*13, 14*), and chemical oxidation (*15*). However in each technique there are limitations and disadvantages. Adsorption involves only phase transfer of pollutants without degradation, chemical oxidation is unable to mineralize all organic substances, and in biological treatment the slow reaction rates and the disposal of activated sludge are the drawbacks to be considered (*16, 17*).

The processes involving light have received increasing attention in the last years because they overcame the above disadvantages. Advanced oxidation processes (AOPs) based on H_2O_2/UV, O_3/UV, and H_2O_2/O_3/UV combinations employ photolysis of H_2O_2 and ozone to produce hydroxyl radicals ($^{\bullet}$OH) that are able to oxidize the pollutants due to their high oxidative capacity (E° = 2.8 V) (*18*). Another interesting AOP is the irradiation of semiconductor slurries by UV light in order to generate highly reactive intermediates, especially $^{\bullet}$OH that initiate a sequence of reactions resulting in partial or total destruction of organic pollutants. Among the semiconductors used (ZnO, TiO_2, and CdS), titanium dioxide has been demonstrated to be a very efficient catalyst and especially suitable to work by solar UV light (*19*). Photoexcitation of semiconductor usually generates an electron−hole pair poised respectively at the conduction and valence edges. The components of this activated pair, when transferred across the interface, are capable of reducing and oxidizing a surface-adsorbed organic compound (*20, 21*). The reaction of this activated pair with the water, and/or with O_2, and/or with hydroxy groups at the semiconductor surface produces high oxidant species ($^{\bullet}$OH radicals, peroxide radicals) which are responsible for a complete oxidative destruction of organic reactants (*22, 23*). Photocatalytic processes using semiconductor particles as catalysts for water purification receive a major interest, especially the last years because of and their efficiency in the mineralization of the aqueous pollutants in a short time and of the adaptability to specially designed reactor systems (*17*).

The present study deals with the photocatalytic degradation of selected s-triazine herbicides and organophosphorus insecticides in the presence of TiO_2 particles (100 mg L^{-1}) and simulated solar light. The objectives were as follows: (i) to determine the main byproducts by using GC-MS techniques in order to propose a degradation pathway and (ii) to evaluate the kinetics of pesticide disappearance. The dependence of the pesticide structure on the degradation rates has been also discussed and new data on the photocatalytic degradation of s-triazine herbicide irgarol and insecticides as bromophos methyl, and dichlofenthion were reported. Atrazine, propazine, and methyl and ethyl parathion were investigated also in other studies (*16, 24, 25*) and were stated as reference compounds for comparison with the photocatalytic degradation of the other selected pesticides belonging to the same chemical groups under the applied experimental conditions.

10.1021/es001271c CCC: $20.00
Published on Web 12/12/2000

TABLE 1. Chemical Structures of Selected Pesticides

s-triazines Herbicides

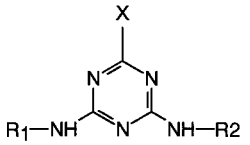

Trivial name	X	R_1	R_2	Chemical name (IUPAC)
Atrazine	Cl	Et	i-Pr	2-chloro-4-ethylamino-6-isopropylamino-1,3,5-triazine
Cyanazine	Cl	Et	i-Pr(CN)	2-chloro-4-(1-cyano-1-methylethylamino)-6ethylamino-1,3,5-triazine
Irgarol	SMe	tert-butyl	cyclopropyl	(2-methylthio-4-tertiary-butylamino-6-cyclopropylamino-s-triazine
Prometryne	SMe	i-Pr	i-Pr	2,4-bis(isopropylamino)-6-methylthio-1,3,5-triazine
Propazine	Cl	i-Pr	i-Pr	2-chloro-4,6-bis(isopropylamino)-1,3,5-triazine

Organophosphorus Insecticides

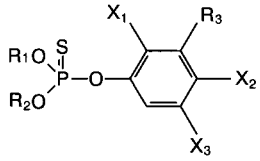

Trivial name	R_1	R_2	R_3	X_1	X_2	X_3	Chemical name (IUPAC)
Dichlofenthion	Et	Et	H	Cl	Cl	H	O-(2,4-dichlorophenyl) O,O-diethyl phosphorothioate
Bromophos Ethyl	Et	Et	H	Cl	Br	Cl	O-4-bromo-2,5-dichlorophenyl O,O-diethyl phosphorothioate
Bromophos Methyl	Me	Me	H	Cl	Br	Cl	O-4-bromo-2,5-dichlorophenyl O,O-dimethyl phosphorothioate
Parathion Ethyl	Et	Et	H	H	NO_2	H	O,O-diethyl O-4-nitrophenyl phosphorothiate
Parathion Methyl	Me	Me	H	H	NO_2	H	O,O-dimethyl O-4-nitrophenyl phosphorothiate

Experimental Section

Chemicals. The tested compounds in this study atrazine, propazine, cyanazine, prometryne, irgarol (s-triazines herbicides), ethyl parathion, methyl parathion, diclofenthion, ethyl bromophos, and methyl bromophos (organophosphorus insecticides) were residue analysis grade and purchased from Riedel-de Häen (Germany) and used without further purification. The chemical structures of these pesticides are shown in Table 1. Pesticide grade *n*-hexane, methanol, dichloromethane, ethyl acetate, and acetone were purchased from Pestiscan (Labscan Ltd., Dublin, Ireland). Sodium chloride and sodium sulfate (proanalysis) was from Merck (Darmstadt, Germany). Titanium dioxide (Degussa P25), a known mixture of 65% anatase and 35% rutile form with an average particle size of 30 nm, nonporous with a reactive surface area (BET) of 50 ± 15 $m^2\ g^{-1}$ was used as received for all degradation experiments. HA 0.45 μm filters were supplied from Millipore (Bedford, USA). SDB (styrene divinylbenzene) extraction disks (47 mm) were purchased from Empore (St. Paul, USA), and a conventional filtration apparatus was purchased from Supelco (Bellefonte, USA).

Irradiation Procedure. Irradiation experiments of s-triazines were carried out on stirred air-equilibrated solutions contained in 4 cm diameter cylindrical Pyrex glass cells. Substrates were dissolved in distilled water at ppm (mg L^{-1}) levels, under their solubility levels by putting the appropriate volume of a stock solution in methanol, to have a methanol content <0.05%. The concentration levels of s-triazines herbicides and organophosphorus insecticides in water were 10 mg L^{-1} and 1 mg L^{-1}, respectively. The concentration of pesticides is high enough to facilitate the identification of intermediate products and in addition should be representative of those found in polluted waters. Ten (*10*) milliliters of the herbicide solution containing the TiO_2 powder (100 mg/L) were magnetically stirred before and during the illumination. The suspension was left for 30 min in the dark in order to achieve the maximum adsorption of pesticides onto semiconductor surface. The degradation of organophosphorus insecticides was carried out in a 100 mL UV-reactor by exposing the appropriate solution volume and TiO_2 amount to the light in order to keep constant, with respect to the previous small cells, the thickness of the solution. For the identification of photoproducts 50 mL of pesticides solution was irradiated separately under the same experimental conditions. The pH of the solutions was not adjusted and was the pH of the Degussa TiO_2 (6.3−6.6).

The irradiation was carried out using a Suntest CPS+ apparatus from Heraeus (Hanau, Germany) equipped with a xenon arc lamp (1500 W) and special glass filters restricting the transmission of wavelengths below 290 nm. The light source was on the top of the reactors used, and an average irradiation intensity of 750 W/m^2 was maintained throughout the experiments, measured by internal radiometer. The corresponding light dose for 10 min of irradiation was 450 kJ/m^2. Chamber and black panel temperature were regulated by pressurized air cooling circuit and monitored using thermocouples supplied by the manufacturer. The temperature of samples did not exceed 35 °C using tap water cooling circuit for the UV-reactor.

Analytical Procedures. At specific time intervals (10 min) samples of 5 mL were withdrawn from the reactor. To remove the TiO_2 particles the solution samples were filtered through 0.45 μm filter. After that, the samples were extracted twice with 2.5 mL of *n*-hexane for one minute using a vortex, dried with a small amount of Na_2SO_4 and finally analyzed by GC, quantified by internal standard. The liquid−liquid extraction is used frequently for routine monitoring analysis of the degradation rates as it is a fast and reliable method for quantification of pesticides in water (*26*, *27*).

For the identification of transformation products the irradiated solution (50 mL) was extracted by means of solid-phase extraction, at the end of total irradiation time, as follows: SDB extraction disks were conditioned with 10 mL of acetone for 2 h, and 5 mL of methanol modifier was added to the residue to allow better extraction. The disks were placed in the filtration apparatus and washed with 5 mL of solvent

mixture, dichloromethane:ethyl acetate (1:1, v/v) under vacuum, and with 3 mL of methanol for 3 min, with no vacuum applied. The disks were not allowed to become dry (*28*), and the samples were allowed to percolate through the disks with a flow rate of 10 mL/min, under vacuum. The compounds trapped in the disks were collected by using 3 × 5 mL of solvent mixture dichloromethane:ethyl acetate (1;1, v/v) as eluting system. The fractions were evaporated to 0.1 mL in a gentle stream of nitrogen, and 2 μL was injected into GC-MS instrument.

The analysis of the s-triazine and organophosphorus compounds was performed using a Shimadzu 14A gas chromatograph equipped with flame thermionic detector (FTD). The DB-1 capillary column, 30 m × 0.32 mm i.d. used contained methylsilicone (J&W Scientific, Folsom, CA) followed a temperature program: 150° C for 2 min, from 150 to 210 °C with a rate of 5 °C/min, at 210 °C for 10 min, 210 to 270 °C with a rate of 10 °C/min, and at 270 °C for 3 min. Helium was used as the carrier and makeup gases. The detector gases were hydrogen and air, and the ion source of FTD was an alkali metallic salt (Rb_2SO_4) bonded to a 0.2 mm spiral of platinum wire. The temperatures were set at 220 °C for the injector and 250 °C for the detector.

For the identification of transformation products a GC-MSD, QP 5000 Shimadzu equipped with DB-5 ms capillary column, 30 m × 0.25 mm i.d. containing 5% phenylsilicone (J&W Scientific, Folsom, CA) was used at the following chromatographic conditions: injector temperature 220 °C, column program of temperatures 55 °C, 55−200 °C (5 °C/min), 200−210 °C (1 °C/min) 210 ºC (*2min*), 210−270 °C (20 °C/min), 270 °C (3 min). Helium was used as the carrier gas at 14 psi. The interface was kept at 270 °C. The spectra were obtained at 70 eV in full scan mode.

Results and Discussion

Photodegradation Kinetics. Several experimental results indicated that the destruction rates of photocatalysis of various organic contaminants over illuminated TiO_2 fitted the Langmuir−Hinshelwood kinetics (*22, 29, 30−33*). The Langmuir−Hinshelwood rate form is

$$v = \frac{dC}{dt} = \frac{kKC}{1 + KC} \quad (1)$$

where v = the oxidation rate of the reactant (mg L^{-1} min^{-1}), C = the concentration of the reactant (mg/L), t = the illumination time, k = the reaction rate constant (min^{-1}), and K = the adsorption coefficient of the reactant onto the TiO_2 particles (L/mg). Integration of eq 1 yields eq 2:

$$\ln\left(\frac{Co}{C}\right) + K(Co - C) = kKt \quad (2)$$

When the initial concentration Co is a millimolar solution (Co small) the eq 2 is altered to the eq 3

$$\ln\left(\frac{Co}{C}\right) = kKt = k't \text{ or } C_t = Coe^{-k't} \quad (3)$$

which express a pseudo-first-order reaction (*17, 29, 34*), where k' is the apparent photodegradation rate constant.

The kinetics of all the investigated pesticides follow an apparent first-order degradation curve which is consistent to the Langmuir−Hinshelwood model resulting from the low coverage of the semiconductor surface in the experimental concentration range from 1 to 10 mg/L (Figures 1 and 2). Tables 2 and 3 list the values of k' and the linear regression coefficients for pseudo-first-order kinetics of the photodegradation of the studied compounds. According to these values the appropriate first-order relationship appears to fit well.

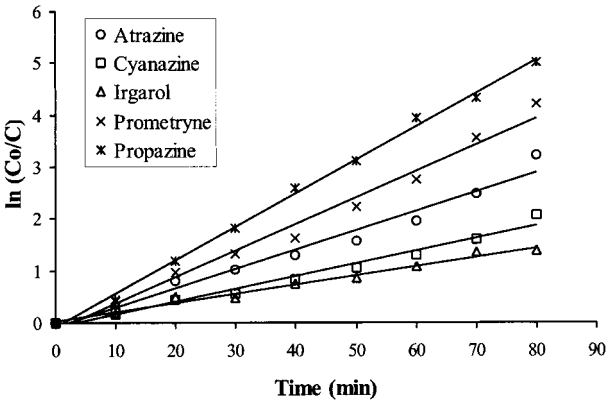

FIGURE 1. Photodegradation rates of s-triazine herbicides (concentration level 10 mg/L) in aqueous TiO_2 suspensions (100 mg/L) under simulated solar light, in the presence of methanol.

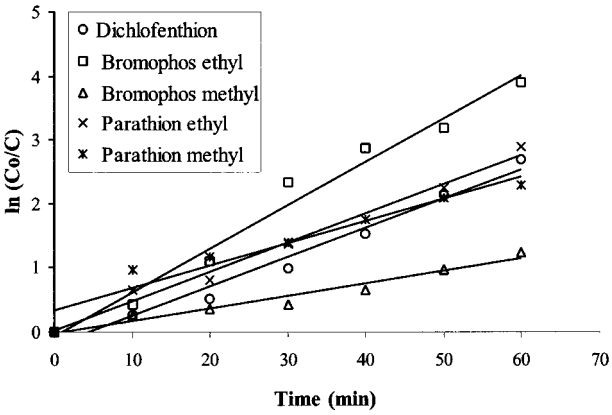

FIGURE 2. Photodegradation rates of organophosphorus insecticides (concentration level 1 mg/L) in aqueous TiO_2 suspensions (100 mg/L) under simulated solar light, in the presence of methanol.

The photolysis (blank experiment without photocatalyst) of the tested pesticides follows also first-order kinetics. The values of the photolysis rate constants (k_{phot}) and the regression coefficients are shown in Tables 2 and 3. As it can be observed from these data the contribution of the direct photolysis in the photodegradation was low or negligible for some compounds (ethyl and methyl parathion, methyl bromophos, atrazine, irgarol, propazine, prometryne), while it was greater for other compounds (ethyl bromophos, cyanazine). To separate the action of the direct photolysis from the photocatalytic oxidation the rate constants of the photocatalytic oxidation (k_{cat}) were calculated by subtracting the constants representing the apparent degradation (k') and the constants representing the photolysis (k_{phot}). In such a way the considered k_{cat} constants refer to the photocatalytic oxidation excluding the contribution of the direct photolysis of the pesticides (Tables 2 and 3).

Adsorption experiments (absence of illumination and presence of catalyst) demonstrated that after the equilibrated adsorption of the pesticides onto the semiconductor surface (30 min), the adsorption did not differ significantly for the reaction time of s-triazines (80 min) and organophosphorus insecticides (60 min). Thus the influence of adsorption on the observed kinetics is not considered to be significant.

All investigated pesticides were sufficiently degraded in aqueous titanium dioxide suspensions, irradiated with simulated solar light. The half-lives ranged from 10.8 to 38.3 min for the studied s-triazines and from 10.2 to 35.5 min for the studied organophosphorus insecticides (Tables 2 and 3).

The rates of the catalytic disappearance depend on various parameters such as initial concentration, radiant flux,

TABLE 2. Photodegradation Kinetic Parameters (Rate Constants, Correlation Coefficients (R^2), Half-Lives ($t_{1/2}$)) of Selected s-Triazines Herbicides, in Distilled Water and in TiO_2 Suspension (100 mg/L), in the Presence of Methanol, Using Simulated Solar Light

	distilled water			TiO_2 (100 mg L^{-1})			
herbicide	$k_{phot.} \times 10^{-3}$ (min^{-1})	R^2	$t_{1/2}$ (min)	$K' \times 10^{-2}$ (min^{-1})	R^2	$t_{1/2}$ (min)	$k_{cat.} \times 10^{-2}$ (min^{-1})
atrazine	1.60	0.96	433.1	3.73	0.97	18.6	3.57
cyanazine	6.40	0.96	108.3	2.44	0.98	28.4	1.80
irgarol	2.00	0.96	346.5	1.81	0.99	38.3	1.61
prometryne	2.30	0.97	301.3	5.10	0.98	13.6	4.87
propazine	1.80	0.98	385.0	6.42	0.99	10.8	6.24

TABLE 3. Photodegradation Kinetic Parameters (Rate Constants, Correlation Coefficients (R^2), Half-Lives ($t_{1/2}$)) of Selected Organophosphorus Insecticides, in Distilled Water and in TiO_2 Suspension (100 mg/L), in the Presence of Methanol, Using Simulated Solar Light

	distilled water			TiO_2 (100 mg L^{-1})			
insecticide	$k_{phot.} \times 10^{-3}$ (min^{-1})	R^2	$t_{1/2}$ (min)	$K' \times 10^{-2}$ (min^{-1})	R^2	$t_{1/2}$ (min)	$k_{cat} \times 10^{-2}$ (min^{-1})
dichlofenthion	6.10	0.96	113.6	4.56	0.98	15.2	3.95
bromophos ethyl	5.01	0.92	138.6	6.80	0.98	10.2	6.29
bromophos methyl	2.90	0.95	239.0	1.95	0.96	35.5	1.66
parathion ethyl	0.70	0.92	990.2	4.56	0.99	15.2	4.49
parathion methyl	0.30	0.95	2310.5	3.46	0.94	20.0	3.43

wavelength, mass and type of photocatalyst, and type of photoreactor; consequently their measurement has no absolute meaning. However for a given set of conditions they allow to compare the photodegradation rates among the different pesticides (or with other organic micropollutants). Comparing the experimental data with previous reported the degradation rates were relatively lower considering the previous mentioned differences in the experimental conditions. Moreover the presence of methanol in the suspension acts competitively, influencing the degradation rate. Pelizzetti and co-workers (*16*) reported that more than 90% of s-triazines compounds was photodegradated within 15 min, using a Xenon arc with $\lambda > 340$ nm. Sanlaville and co-workers (*35*) also reported full decomposition of s-triazines within 30 min using Suntest apparatus ($\lambda > 290$ nm).

Comparison of Photocatalytic Oxidation Constants. It is well established that conduction band electrons (e^-) and valence band holes (h^+) are generated when aqueous TiO_2 suspension is irradiated with light energy greater than its band gap energy (e.g. 3.2 eV). The photogenerated electrons could reduce the organic substrate or react with the adsorbed molecular O_2 on the Ti(III)-surface, reducing it to superoxide radical anion $O_2^{\bullet -}$. The photogenerated holes can also oxidize either the organic molecules directly or the OH^- ions and the H_2O molecules adsorbed at the TiO_2 surface to $^{\bullet}OH^{\bullet}$ radicals. Together with other highly oxidant species (peroxide radicals) they are reported to be responsible for the heterogeneous TiO_2 photodecomposition of organic substrates. According to this, the relevant reactions at the semiconductor surface can be expressed as follows:

$$TiO_2 + h\nu \rightarrow e^- + h^+ \quad (4)$$

$$(O_2)_{ads.} + e^- \rightarrow (O_2^{\bullet -})_{ads.} \quad (5)$$

$$Ti(IV)\text{-}OH + h^+ \rightarrow Ti(IV)\text{-}OH^{\bullet} \quad (6)$$

$$Ti(IV)\text{-}H_2O + h^+ \rightarrow Ti(IV)\text{-}OH + H^+ \quad (7)$$

$$R + h^+ \rightarrow R\ (oxidized) \quad (8)$$

$$R + OH^{\bullet} \rightarrow products \rightarrow \ldots \quad (9)$$

The photocatalytic oxidation rate constants depends on the structure of the tested pesticides mainly in the early part of the irradiation experiments, up to 20 min. The reaction types of the hydroxy radical with organic compounds include only two of significant importance: electron or hydrogen atom abstraction and addition to double bonds (*36*). In the case of s-triazines different initial rates were observed but for prometryne, atrazine, and propazine similar degrees of degradation were reached finally. This fact demonstrates that the initial rate, although useful, can be misleading when used as the only piece of information to estimate the efficiencies of the photocatalytic degradation of a series of pollutants. The above result could be explained comparing the alkyl substituents in the lateral chains and the substituent in the position two of the aromatic ring. The first reaction which takes place is the oxidation of the lateral chains, and the main degradation products were the acetamido and dealkylated derivatives which is consistent to what is reported elsewhere (*24*, *35*). The followed reactions were the photohydrolysis of the substituent in the position two and the final displacement of the amino with hydroxy groups (*16*). The rate constants for the 2-chloro s-triazines increases in the order propazine> atrazine > cyanazine. This order was reasonable considering that the hydrogen abstraction by the produced OH· radicals was the low step of the reaction followed by the very fast reaction with O_2 through the formation of peroxy radicals as reported elsewhere (*37*). In other previously investigated photocatalytic processes the crucial importance of O_2 was assessed (*16*). Although OH· radicals are very unselective, in practice there is some discrimination among potential sites of attack (*36*). The lower ionization potential of the amine at position 4 compared with the amine at position 6 might explain the above observation (*37*). Considering the stability of the different possible *N*-ethyl and *N*-isopropyl radicals that could take part in the reaction, this explanation can also be supported.

Similar results were observed comparing the two methylthio s-triazines (prometryne > irgarol). When comparing the methylthio triazines with the chloro-triazines (i.e. propazine and prometryne) the rate of photoreactions was affected by the electronegativity of the substituent at position 2 which interferes through the aromatic ring with the stability

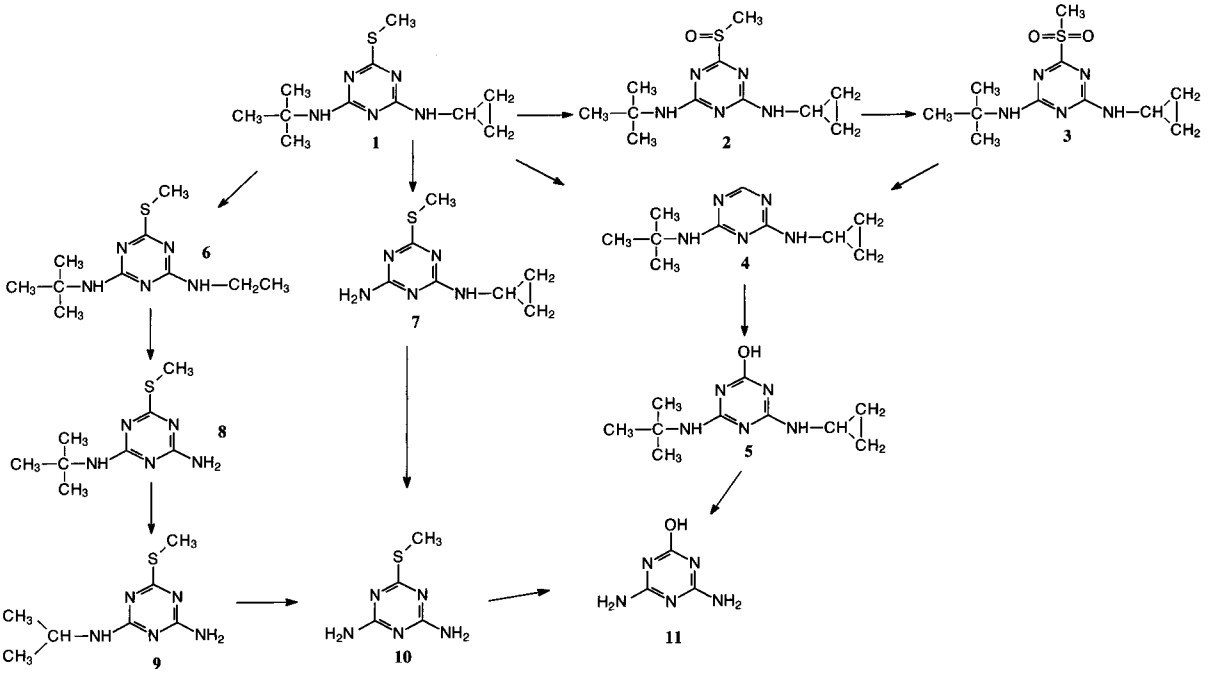

FIGURE 3. Proposed photodegradation pathway of irgarol in aqueous TiO_2 suspensions under simulated solar light.

of substituents at position 4 and 6 (*37*). The decrease of the reaction rate in the order $-Cl > -SCH_3$ could be explained by the two-step mechanism of $-SCH_3$ oxidation according to the reaction scheme (Figure 3) discussed below.

Photocatalytic oxidation rate constant comparison of organophosphorus insecticides (Table 3) indicates that the compounds with the ethoxy group degraded faster than compounds possessing methoxy groups. This observation is also supported considering the stability of the different possible dialkyl-phosphate radicals that were formed during the reaction. Alkyl groups have an inductive effect to release electrons. The effect overlaps with the pπ-dπ contribution of lone pair electrons on the oxygen of the ester group and is increased in the following order: methyl < ethyl (*38*). Thus, half-lives of ethoxy compounds (ethyl parathion, ethyl bromophos) were found 15.2 and 10.2 min instead of 20 and 35 min for the methoxy analogues (methyl parathion, ethyl parathion), respectively.

Irgarol Photodegradation Pathway. Based on the previous observations on the reaction behavior of thioethers in the presence of TiO_2 and UV irradiation (*39*), the photogenerated hole localized at the surface of the irradiated semiconductor is trapped by an adsorbed organosulfur compound, generating an adsorbed cation radical. This localization of positive charge at sulfur would be expected either in the transition state, leading to the initial oxygen adduct, or by Bronsted or Lewis acid complexation, respectively, with acidic or Ti^{4+} sites on the metal oxide surface. Based on the above consideration the analogue mechanism for the oxidation of irgarol $-SCH_3$ group is proposed in Figure 4. The reaction scheme displayed in Figure 3 is proposed for irgarol (compound **1**) photocatalytic oxidation. The mass spectra of some irgarol photoproducts appeared here for the first time, and their spectral characteristics and retention times are given in Table 4. According to the above scheme the degradation in the early steps is progressed through competitive reactions such as oxidation of the side alkyl chains and oxidation of irgarol's sulfur atom by $^{\bullet}OH$ and O_2 or superoxide attack. Some of the primary products formed during photocatalysis were the sulfone (compound **3**) and sulfoxide (compound **2**) derivatives (Figure 3). Further reaction implies the cleavage of the sulfur group from the

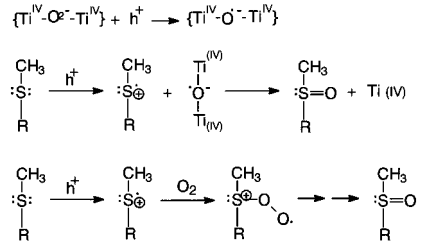

FIGURE 4. Proposed reaction scheme for the photooxidation of thiomethyl group of irgarol in aqueous solutions by TiO_2 and simulated solar light, describing the formation of transformation products 2 and 3 in the proposed photodegradation pathway of irgarol (Figure 3).

triazine ring resulting in the formation of compound **4** and the hydroxylated compound **5**. This is in agreement with mechanisms proposed by other groups for another methylthio triazine such as prometryne (*40*, *15*). The second possible route is the oxidation of the alkylic side chains attached to the nitrogen atoms in position 4 and 6 leading to the formation of the dealkylated derivatives (compounds **6**−**10**). The mechanism of degradation from compound **8** to **9** suggests the possible participation of peroxide radicals. The radical formed by hydrogen abstraction from a methyl group of the *tert*-butyl chain could be expected to react with the dissolved oxygen to yield peroxide radicals which after decarboxylation produce the dealkylated analogue (*41*). Although that quantitative determination of byproducts was not realized because of unavailable standards, the higher relative abundance of compounds **7**−**9** compared to the other identified compounds revealed that the last process was the main pathway and occur approximately for 90% of photodegradation. This observation is in accordance with results referred to the photocatalytic degradation of 2-Cl-triazines proposed by other researchers (*16*, *24*, *35*). Further oxidation leads to the formation of hydroxy and dealkylated derivative as ammeline (compound **11**) which is an identified photoproduct in photocatalysis of all s-triazine herbicides.

Dichlofenthion and Bromophos Photodegradation Pathway. Oxidant attack of the $^{\bullet}OH$ on the P═S bond occurred first in the case of dichlofenthion and bromophos, resulting

TABLE 4. GC-MS-EI Retention Times (R_t) and Spectral Characteristics of Irgarol Major Photoproducts

herbicide-photoproducts	R_t (min)	EI-MS spectrum (*m/z*) ions
(**1**)[a] Irgarol 1051 (2-methylthio-4-terbutylamino-6-cyclopropylamino-s-triazine)	36.84	253 (M^+), 238, 196, 182, 109, 83, 56
(**2**) 2-methylsulfinyl-4-terbutylamino-6-cyclopropamino-s-triazine	41.09	269 (M^+), 254, 213, 198, 157, 129, 73
(**3**) 2-methylsulfonyl-4-terbutylamino-6-cyclopropamino-s-triazine	42.69	286 (M^+), 253, 238, 196, 159, 182, 111, 83
(**4**) 4-terbutylamino-6-cyclopropylamino-s-triazine	26.36	207 (M^+), 192, 150, 136, 123, 96, 83, 56
(**5**) 2-hydroxy-4-terbutylamino-6-cyclopropylamino-s-triazine	29.71	223 (M^+), 209, 194, 179, 112, 91, 69
(**6**) 2-methylthio-4-amino-6-(ethylamino)-s-triazine	36.27	241 (M^+), 226, 213, 198, 185, 157, 111, 83, 68
(**7**) 2-methylthio-4-amino-6-cyclopropylamino-s-triazine	32.61	197 (M^+), 182, 127, 109, 83, 68
(**8**) 2-methylthio-4-terbutylamino-6-amino-s-triazine	30.24	213 (M^+), 198, 157, 149, 111, 99, 83, 68
(**9**) 2-methylthio-4-isopropylamino-6-amino-s-triazine	34.28	199 (M^+), 157, 111, 68
(**10**) methylthiodiamino-s-triazine	26.83	157 (M^+), 111, 69, 68
(**11**) diaminohydroxy-s-triazine	13.03	128 (M^+), 97, 83, 69, 55

[a] Corresponding number in the proposed pathway of Figure 3.

TABLE 5. Identified Photoproducts in Dichlofention and Ethyl Bromophos Photocatalytic Degradation and Their Main Fragments Determined by GC-MS in the EI Mode

insecticide-photoproducts	R_t (min)	EI-MS spectrum (*m/z*) ions
(**1**)[a] methyl bromophos	34.72	333, 331, 329, 125, 109, 97, 93, 79
(**2**) methyl bromooxon	32.78	348 (M^+), 350, 352, 315, 313, 242, 240, 109, 96, 79
(**3**) 4-bromo-2,5-dichlorophenol	20.49	242, 240 (M^+), 135, 133, 99, 97, 96, 81, 79, 73
(**4**) *O,O,O*-trimethyl phosphorothioate	9.22	156 (M^+), 126, 125, 109, 93
(**5**) 3-chlorophenol	10.70	130, 128 (M^+), 100, 99, 92, 75, 65
(**1**)[a] dichlofenthion	30.88	314 (M^+), 281, 279, 253, 251, 225, 223, 164, 162, 125, 109, 97, 88
(**2**) dichlofenoxon	29.10	298 (M^+), 265, 263, 237, 235, 209, 207, 164, 162, 127, 109, 99, 81
(**3**) 2,4-dichlorophenol	12.40	164, 162 (M^+), 126, 100, 99, 98, 63
(**4**) *O,O*-diethyl *O*−*p*-chlorophenyl phosphorothioate	30.68	281 (M^+), 279, 253, 251, 225, 223, 164, 162, 133, 125, 109, 97, 88
(**5**) 4-chlorophenol	10.20	130, 128 (M^+), 100, 99, 93, 92, 65,
(**6**) *S*-ethyl dichlofenthion	33.91	314 (M^+), 281, 279, 253, 251, 225, 223, 164, 162, 125, 109, 97
O,O,O-triethyl phosphorothioate	15.65	198 (M^+), 170, 153, 142,138, 125, 111, 110, 109, 97
diethyl dithiophosphate	17.53	186 (M^+), 158, 153, 142, 125, 121, 109, 97
O,O-diethyl *O*-methyl phosphate	14.71	168 (M^+), 140, 138, 123, 110, 109, 91, 81
O,O-diethyl *O*-methyl phosphorothioate	14.00	184 (M^+), 156, 140, 128, 124, 111, 98, 95, 79
diethyl acid phosphite	6.36	138 (M^+), 111, 110, 109, 93, 83, 65

[a] Corresponding number in the proposed pathway of Figures 5 and 6.

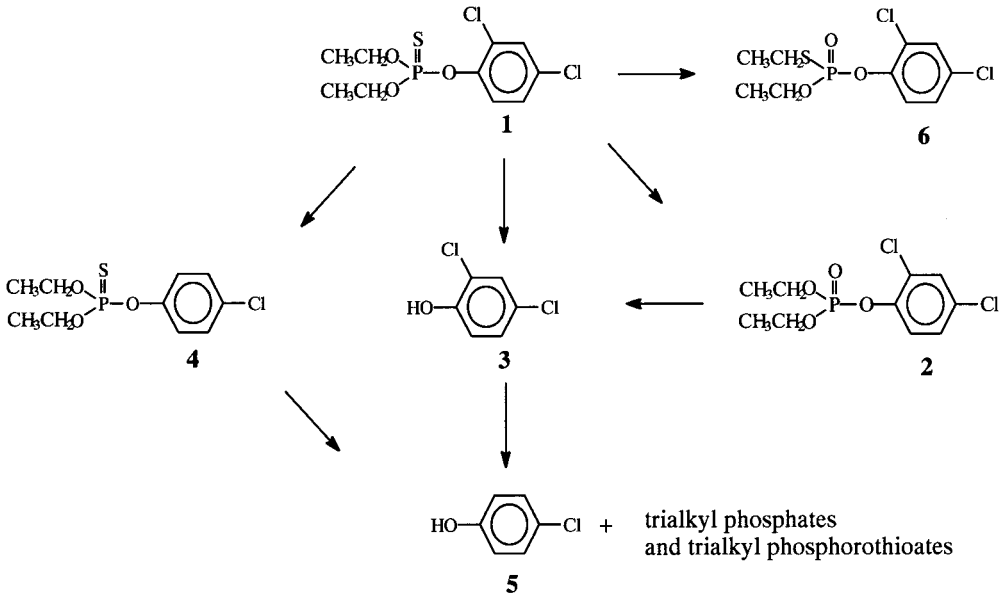

FIGURE 5. Proposed photodegradation pathway of dichlofenthion in aqueous solutions by TiO_2 and simulated solar light.

the formation of oxon derivatives (bromoxon and dichlofenoxon) which are also characteristic primary products formed during the photocatalytic degradation of other organophosphorus insecticides (*42*). The continuous attack of •OH followed by the rupture of P−O bond resulted in the formation of the corresponding phenol and dialkyl-phosphates (*43*). The photoproducts together with their retention times and spectral characteristics are given in Table 5. According to this structure identification the proposed reaction pathways for dichlofenthion and bromophos methyl are shown in Figures 5 and 6, respectively.

For dichlofenthion compound **6** was identified as its *S*-ethyl isomer dichlofenthion. Its spectrum (*6*) has common features with that of dichlofenthion with slightly stronger M^+ intensity, more abundant $m/z = 125$ fragment ion, and weaker intensities in the rest common ions (*44*). Especially

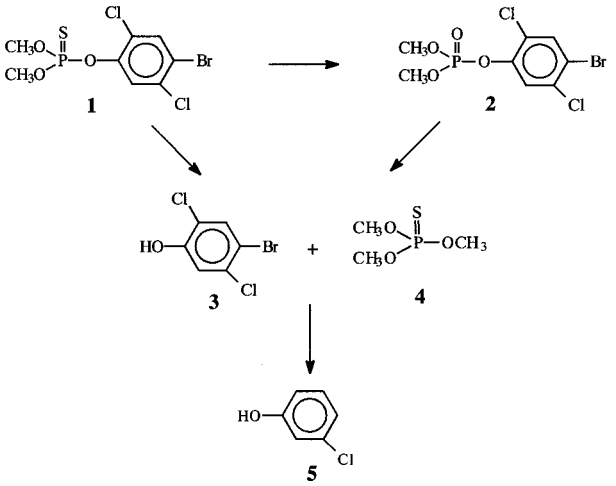

FIGURE 6. Proposed photodegradation pathway of bromophos methyl in aqueous solutions by TiO_2 and simulated solar light.

the fragment ion $m/z = 109$ has distinguishable lower intensity at *S*-ethyl dichlofenthion spectrum than its parent compound spectrum. This observation reported elsewhere on the explanation of mass spectrum of isomeric compound *O*,*S*-diethyl-phenyl phosphorothioate (*45*). Finally the *S*-ethyl isomer of dichlofenthion exhibits longer retention time than dichlofenthion (*46*). Measurable amounts of different trialkyl and dialkyl phosphorothioate or phosphate esters were formed. The characteristic mass spectra data of these products are listed in Table 5 and were well established in previous reported studies of organophosphorus insecticides photodegradation. The photolytic conversion of ethyl parathion into similar structured triethyl phosphorothioates upon solution irradiation with UV-light has been reported also elsewhere (*47*).

In conclusion, effective destruction of the selected pesticides, present at ppm level in water or wastewater, is possible by photocatalysis in the presence of TiO_2 suspensions. The potential of using sunlight as energy source in the photocatalytic process is particularly relevant for Mediterranean agricultural areas, where solar irradiation is highly available making this process quite attractive.

The great number of compounds detected during the degradation of the above compounds shows the complexity of the photocatalytic process and suggests the existence of various degradation routes resulting in complex and interconnected pathways. Cost-effective treatments to complete compound mineralization are usually not practicable, and the presence of byproducts during and at the end of the water treatment appears to be unavoidable (*48*). Therefore, byproduct evaluation is the key to optimize each treatment and to maximize the overall process. The identification of possible formation of highly toxic compounds (as the oxon derivatives for the organophosphorus insecticides) even at low concentrations is essential for the assessment of treated water. Furthermore, the evaluation of the pesticide degradation degree achieved after treatment is necessary.

However, most of the studies on the photocatalytic degradation of pesticides relies only on the evaluation of the disappearance of the initial pollutant combined with monitoring total organic carbon (TOC) plus inorganic ions (Cl^-, NH_4^+, SO_4^{2-} etc). Obviously this is not useful in the case of real waters or when commercial pesticide formulations are treated as a consequence of the presence of other sources of ions and organic compounds.

Supporting Information Available

Figures of GC-MS-EI spectra of irgarol, dichlofenthion, and bromophos methyl photoproducts and GC-MS-EI chromatograms of irgarol, dichlofenthion, and bromophos methyl. This material is available free of charge via the Internet at http://pubs.acs.org.

Literature Cited

(1) Durand, G.; Barcelo, D. *J. Chromatogr.* **1990**, *502*, 275−286.
(2) Ferrer, I.; Barcelo, D. *J. Chromatogr.* **1999**, *854*, 197−206.
(3) Readman, J. W.; Wee Kwong, L. L.; Grondin, D.; Bartocci, J.; Villeneuve, J. P.; Mee, L. D. *Environ. Sci. Technol.* **1993**, *27*, 1940−1942.
(4) Tolosa, I.; Readman, J. W.; Blaevoet, A.; Ghilini, S.; Batrocci, J.; Horvat, M. *Mar. Pollut. Bull.* **1996**, *32*, 335−341.
(5) Scarlett, A.; Donkin, P.; Fileman, T. W.; Morris, R. J. *Mar. Pollut. Bull.* **1999**, *38*, 687−691.
(6) Toth, S.; Becker-van Slooten, K.; Spack, L.; de Alencastro, L. F.; Tarradellas, *J. Bull. Environ. Contam. Toxicol.* **1996**, *57*, 426−433.
(7) Lacorte, S.; Jeanty, G.; Marty, J. L.; Barcelo D. *J. Chromatogr.* **1997**, *777*, 99−114.
(8) Durand, G.; De Bertrand, N.; Barcelo, D. *J. Chromatogr.* **1991**, *554*, 233−250.
(9) Albanis, T. A.; Hela, D. G.; Sakellarides, T. M.; Konstantinou, I. K. *J. Chromatogr.* **1998**, *823*, 59−71.
(10) Pollard, S. J. T.; Fowler, G. D.; Sollars, C. J.; Perry, R. *Sci. Total Environ.* **1992**, *116*, 31−52.
(11) Banerjee, K.; Cheremisinoff, P. N.; Cheng, S. L. *Environ. Sci. Technol.*, **1995**, *29*, 2243−2251.
(12) O'Brien, G. J. *Water Environ. Res.* **1992**, *64*, 877−883.
(13) Somich, C. J.; Muldoon, M. T.; Kearney, P. C. *Environ. Sci. Technol.* **1990**, *24*, 745−749.
(14) Nyholm, N.; Jakobsen, B. N.; Pedersen, B. M.; Poulsen, O.; Damborg, A.; Schulz, B. *Water Res.* **1992**, *26*, 339−353.
(15) Mascolo, G.; Lopez, A.; Foldenyi, R.; Passino, R.; Tiravanti, G. *Environ. Sci. Technol.* **1995**, *29*, 2987−2991.
(16) Pelizzetti, E.; Maurino, V.; Minero, C.; Carlin, V.; Pramauro, E.; Zerbinati, O.; Tosato, M. *Environ. Sci. Technol.* **1990**, *24*, 1559−1565.
(17) Wang, K. H.; Hsieh, Y. H.; Chou, M. Y.; Chang, C. Y.; *Appl. Catal. B: Environ.* **1999**, *21*, 1−8.
(18) Zwiener, C.; Weil, L.; Niessner, R. *Intern. J. Anal. Chem.* **1995**, *58*, 247−264.
(19) Pelizzetti, E. *Solar Ener. Mater. Solar Cells* **1995**, *38*, 453−461.
(20) Pelizzetti, E.; Pramauro, E.; Minero, C.; Serpone, N.; Borgarello, E. In *Photocatalysis and Environment-Trends and applications*; NATO ASI Series, Schiavello, M., Eds.; Kluwer: Dordrecht, The Netherlands, 1988; pp 469−497.
(21) Ollis, D. F.; Pelizzetti, E.; Serpone, N. In *Photocatalysis: Fundamental and Applications*; Serpone, N., Pelizzetti, E., Eds.; Wiley: New York, 1989; pp 603−637.
(22) Turchi, C. S.; Ollis, D. F. *J. Catalysis* **1989**, *119*, 483−496.
(23) Childs, L. P.; Ollis, D. F. *J. Catalysis* **1980**, *66*, 383−390.
(24) Pelizzetti, E.; Carlin, V.; Minero, C.; Pramauro E.; Vinceti M. *Sci. Total Environ.* **1992**, *123/124*, 161−169.
(25) Chen, T. F.; Doong, R.; Lei, W. G. *Water Sci. Technol.* **1998**, *37*, 187−194.
(26) Sanz-Asensio, J.; Plaza-Medina, M.; Martinez-Soria, M. T.; Perez-Clavijo, M. *J. Chromatogr. A* **1999**, *840*, 235−247.
(27) Penuela, G. A.; Barcelo D. *TrAC Trends Anal. Chem.* **1999**, *840*, 235−247.
(28) Lacorte, S.; Molina, C.; Barcelo, D. *Anal. Chim. Acta* **1993**, *281*, 71−84.
(29) D'Oliveira, J. C.; Al-Sayyed, G.; Pichat, P. *Environ. Sci. Technol.* **1990**, *4*, 990−996.
(30) Ollis, D. F.; Hsiao, C. Y.; Budiman, L.; Lee, C. L. *J. Catalysis* **1984**, *88*, 89−96.
(31) Okamoto, K. I.; Yamamoto, Y.; Tanaka, H.; Itaya, A. *Bull. Chem. Soc. Jpn.* **1985**, *58*, 2023−2028.
(32) Al-Ekabi, H.; Serpone, N. *J. Phys. Chem.* **1988**, *92*, 5726−5731.
(33) Topalov, A.; Molnar-Gabor, D.; Csanadi, J. *Water Res.* **1999**, *33*, 1371−1376.
(34) Moza, P. N.; Hustert, K.; Pal, S.; Sukul, P. *Chemosphere* **1992**, *11*, 1675−1682.
(35) Sanlaville, Y.; Guittonneau, S.; Mansour, M.; Feicht, E. A.; Meallier, P.; Kettrup, A. *Chemosphere* **1996**, *33*, 353−362.
(36) Larson, R. A.; Weber, E. J. *Reaction mechanisms in environmental organic chemistry*; CRC Press: Boca Raton, FL, 1994; pp 217−261.
(37) Rejto, M.; Saltzman, S.; Acher, A. J.; Muskat, L. *J. Agric. Food Chem.* **1983**, *31*, 138−143.
(38) Eto, M. *Organophosporus pesticides: Organic and biological chemistry*; CRC Press: Cleveland, U.S.A., 1974; p 63.

(39) Fox, M. A.; Abdel-Wahad, A. A. *Tetrahedron Lett.* **1990**, *31*, 4533−4536.
(40) Borio, O.; Gawlik, B. M.; Bellobono, I. R.; Muntau, H. *Chemosphere* **1998**, *37*, 975−989.
(41) Pelizzetti, E.; Minero, C.; Carlin, V.; Vincenti M.; Pramauro, E.; Dolci, M. *Chemosphere* **1992**, *24*, 891−910.
(42) Kerthentsev, M.; Guillard, C.; Hermann, J. M.; Pichat P. *Catalysis Today* **1996**, *27*, 215−220.
(43) Pignatello, J. J.; Sun, Y. *Water Res.* **1995**, *29*, 1837−1844.
(44) Wilkins, J. P. G. *Pest. Sci.* **1990**, *29*, 163−181.
(45) Desmarchelier, J. M.; Wustner, D. A.; Fukuto T. R. *Residue Rev.* **1976**, *63*, 77−185.
(46) Durand, G.; Mansour, M.; Barcelo, D. *Anal. Chim. Acta* **1992**, *262*, 167−178.
(47) Chukwudebe, A.; March, R. B.; Othman, M.; Fukuto, T. R. *J. Agric. Food Chem.* **1989**, *37*, 539−545.
(48) Herrmann, J. M.; Guillard, C.; Arguello, M.; Aguera, A.; Tejedor, A.; Piedra, L.; Fernadez-Alba, A. *Catalysis Today* **1999**, *54*, 353−367.

Received for review May 16, 2000. Revised manuscript received September 11, 2000. Accepted October 24, 2000.

ES001271C